Electronic Supplementary Information (ESI)

Skin-Breathable and Stretchable Electrode Based on Square-Shaped AgNW Bundle Mesh with Wavy Bridges

Eun Young An[1,2,†], Siyoung Lee[3,†], Jeong Ho Cho[2], Geun Yeol Bae[4,*], and Gyojic Shin[1,*]

E. Y. An and Dr. G. Shin
[1] Green and Sustainable Materials R&D Department, Korea Institute of Industrial Technology, Cheonan 31056, Korea

E. Y. An and Prof. J. H. Cho
[2] Department of Chemical and Biomolecular Engineering, Yonsei University, Seoul 03722, Korea

Dr. S. Lee
[3] Department of Mechanical and Industrial Engineering, University of Toronto, Toronto M5S 3G8, Canada

Prof. G. Y. Bae
[4] Department of Material Design Engineering, Kumoh National Institute of Technology, Gumi 39177, Kore

* Correspondence: gyshin@kitech.re.kr (G.S.), gybae@kumoh.ac.kr (G.Y.B.)

† These authors contributed equally to this work.

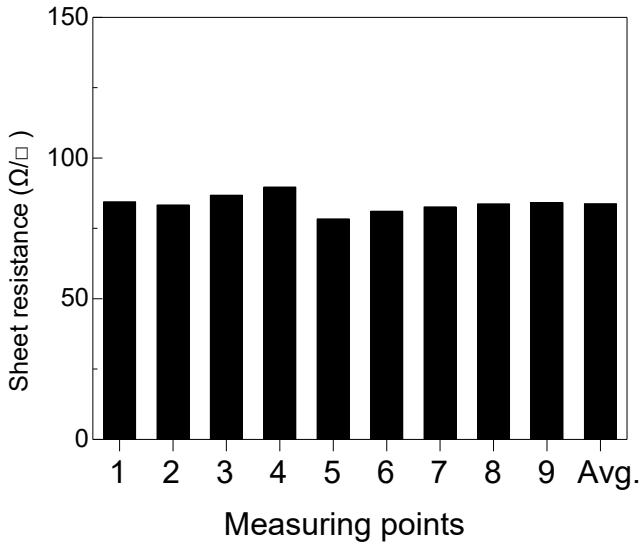

Figure S1. Sheet resistance values of the developed electrode (The size: 2.5 cm × 2.5 cm) depending on various measuring points. The standard deviation for all points is 3.02 Ω □−1.

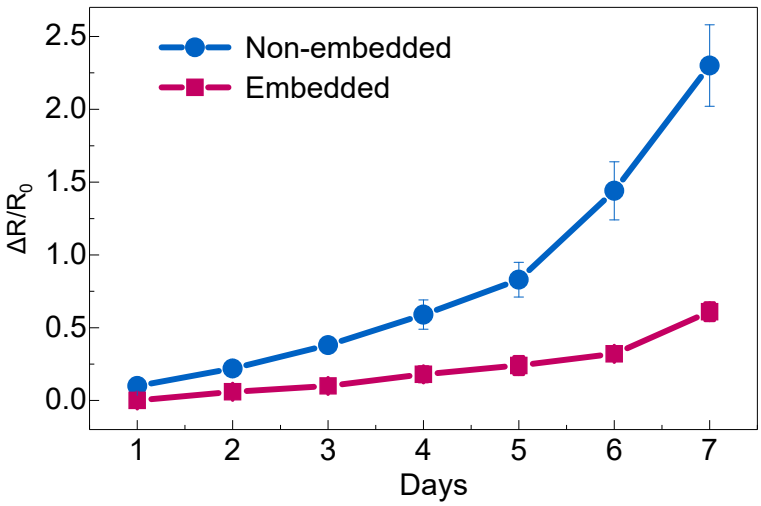

Figure S2. The relative resistance change ($\Delta R/R_0$) in the stretchable electrode (Embedded) and bare silver nanowires (AgNWs) (Non-embedded) during 7 days at a constant temperature (23 °C) and humidity (30 %). The bare AgNWs were obtained by spray-coating AgNWs dispersion on microstructured PDMS substrate. The reference point (i.e., 0.0) of $\Delta R/R_0$ corresponds to initial resistance just after the fabrication.

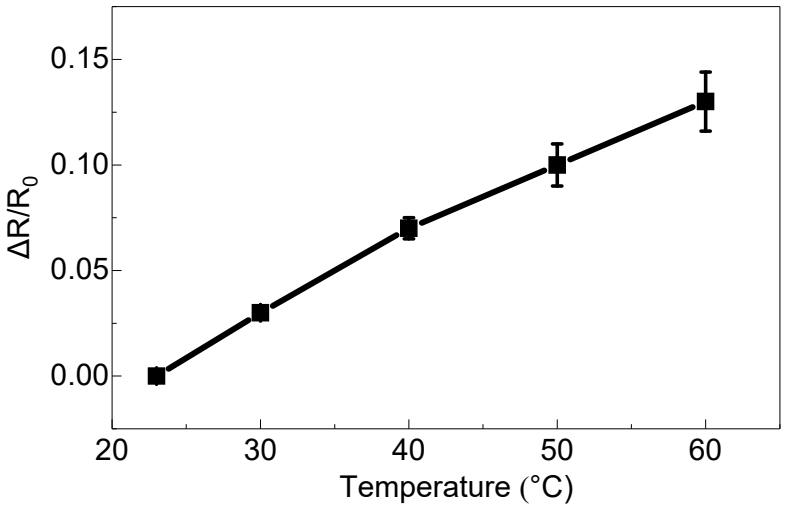

Figure S3. The relative resistance change ($\Delta R/R_0$) in the stretchable electrodes at temperatures from room temperature (23 ℃) to 60 ℃. The reference point (i.e., 0) of $\Delta R/R_0$ corresponds to the resistance at the room temperature.

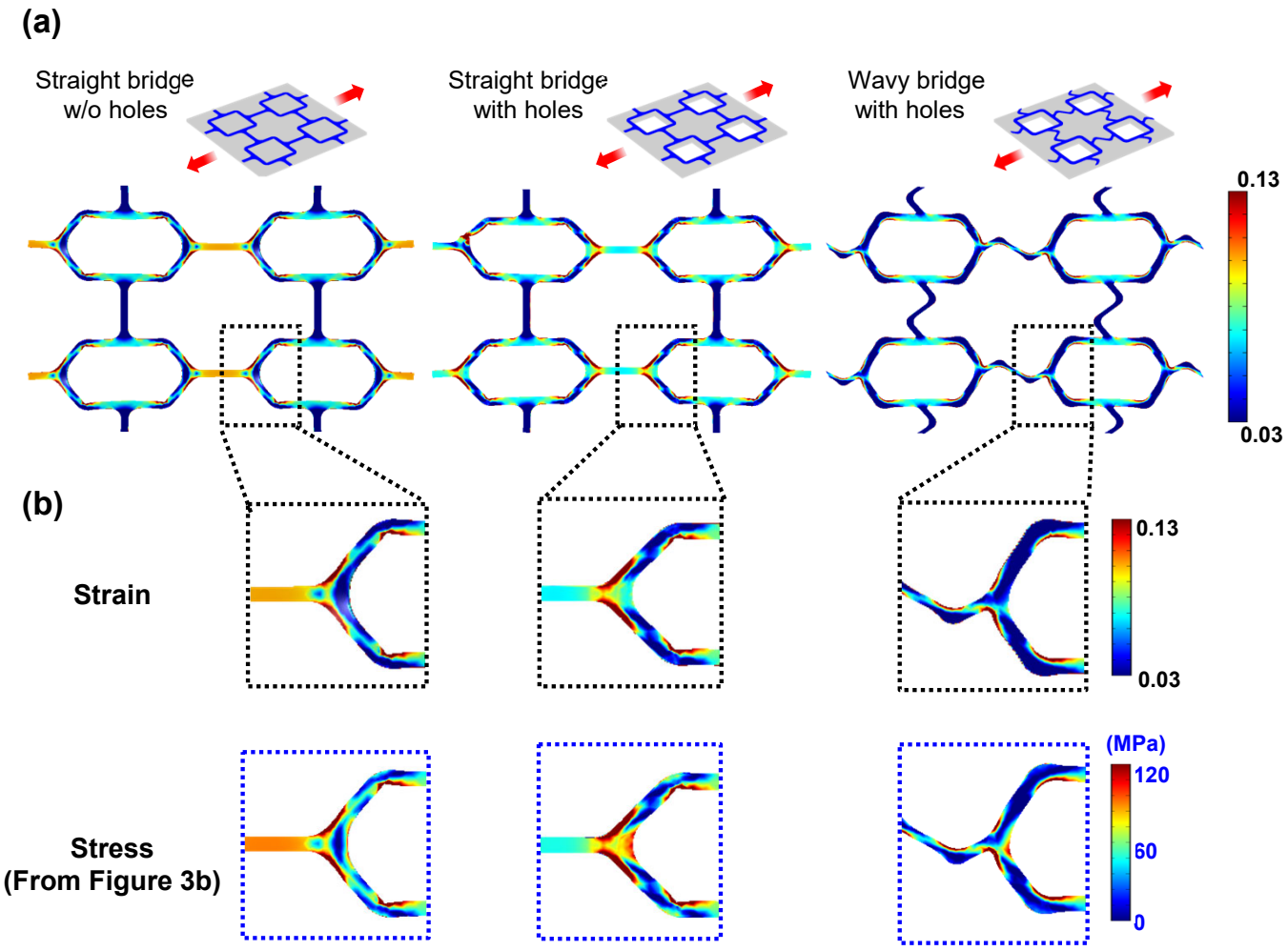

Figure S4. (a) Simulation data of the strain and deformation of stretchable electrodes depending on the hole array and the structure of bridges under 30 % stretching. (b) The comparison of the strain and stress (Figure 3b) results. The distributions of magnitudes for the strain and the stress are identical at bridges and square mesh structures but have a slight difference at the connection points between the bridges and the square meshes. Additional stress is applied to the connection points due to the compressive deformation of AgNW bundles.

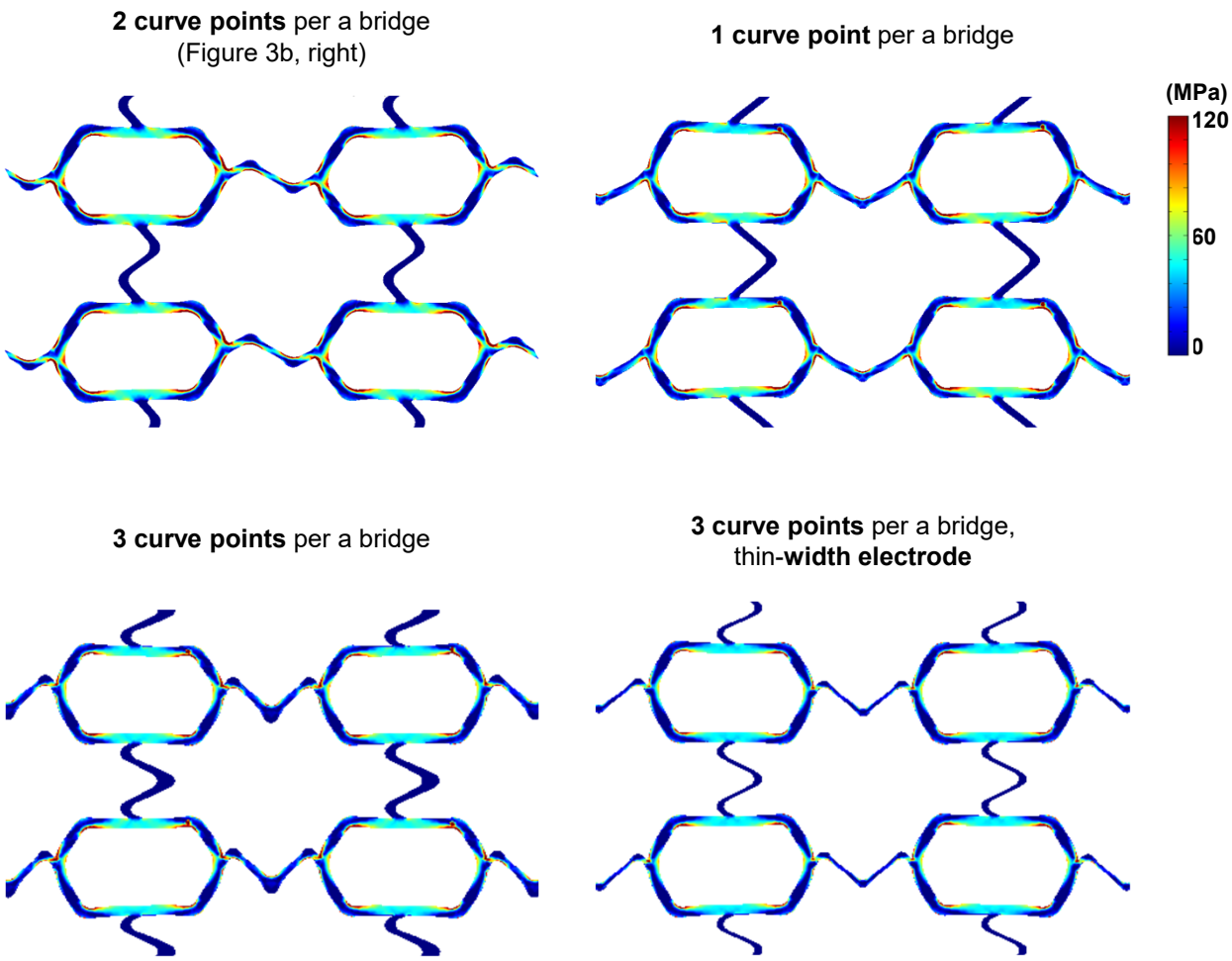

Figure S5. Simulation data of the stress distribution and deformation of stretchable electrodes under 30 % stretching, depending on the curve points and width of wavy bridges.

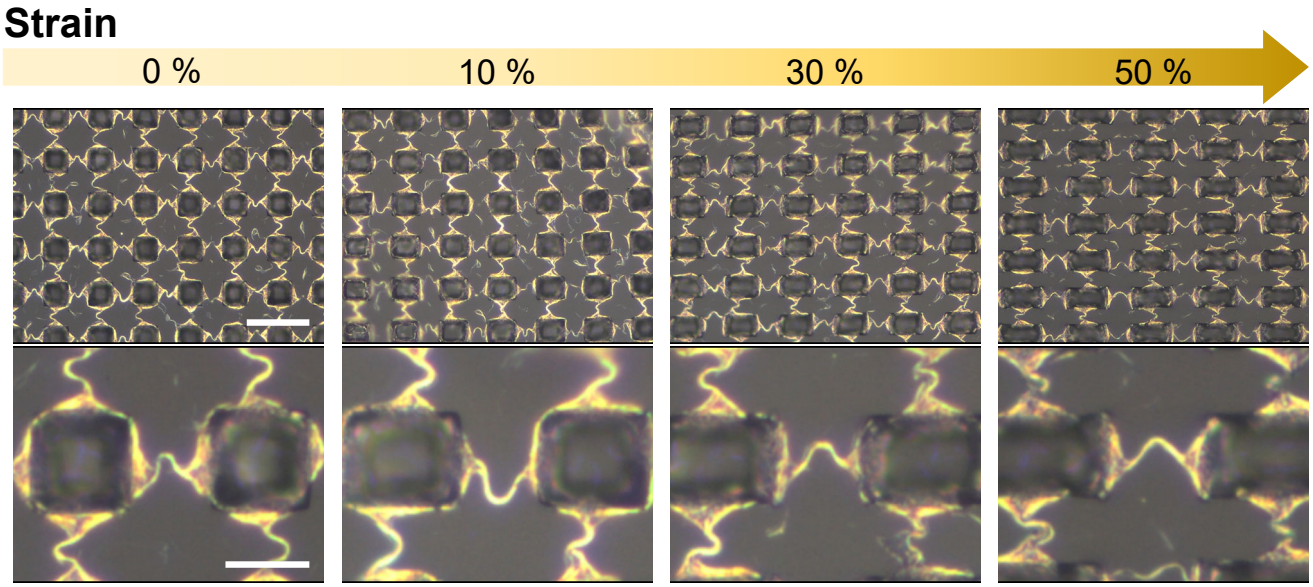

Figure S6. Optical images of the stretchable electrode depend on 10, 30, and 50 % strain. Top (Scale bar: 30 μm) and bottom (Scale bar: 10 μm) images show a wavily bridged silver nanowire micromesh array and a wavy silver nanowire bridge, respectively.

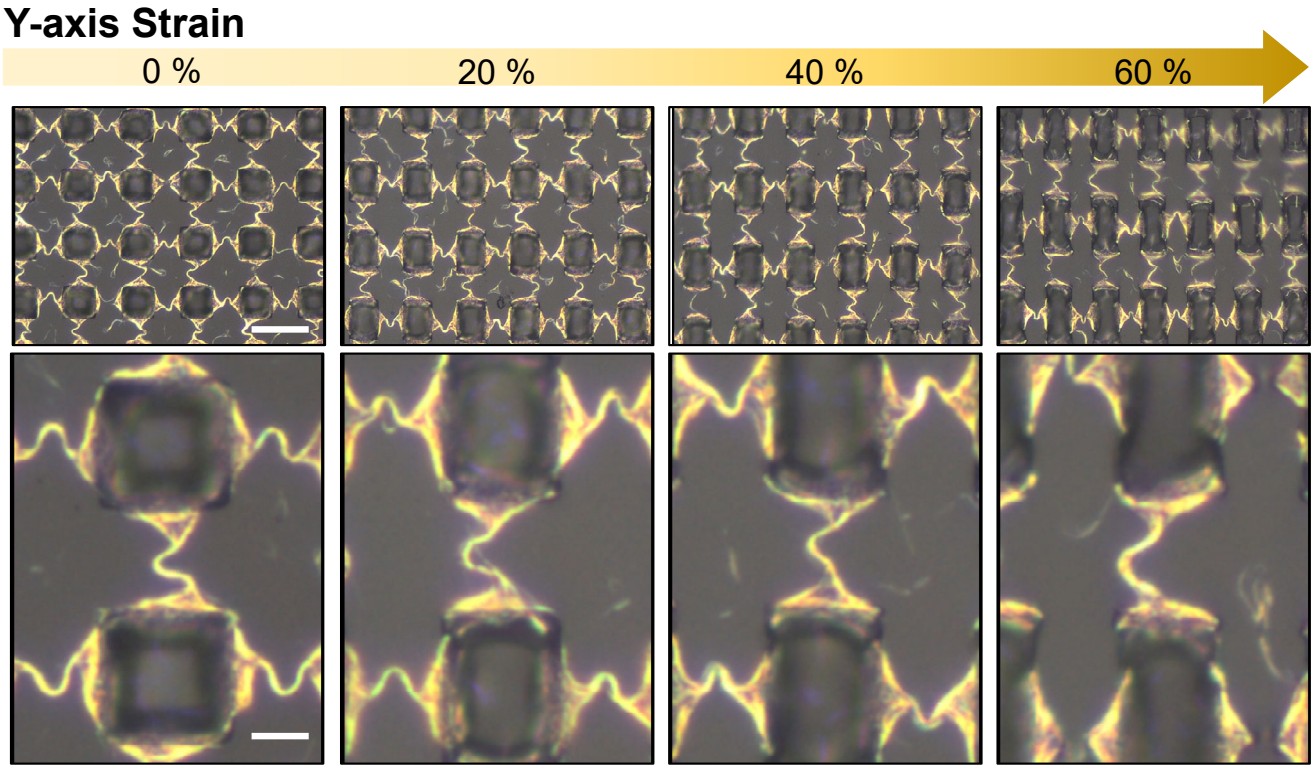

Figure S7. Optical images of the stretchable electrode depending on the Y-axis strain of 20, 40, and 60 %. Top (Scale bar: 20 μm) and bottom (Scale bar: 5 μm) images show a wavily bridged silver nanowire micromesh array and a wavy silver nanowire bridge, respectively.

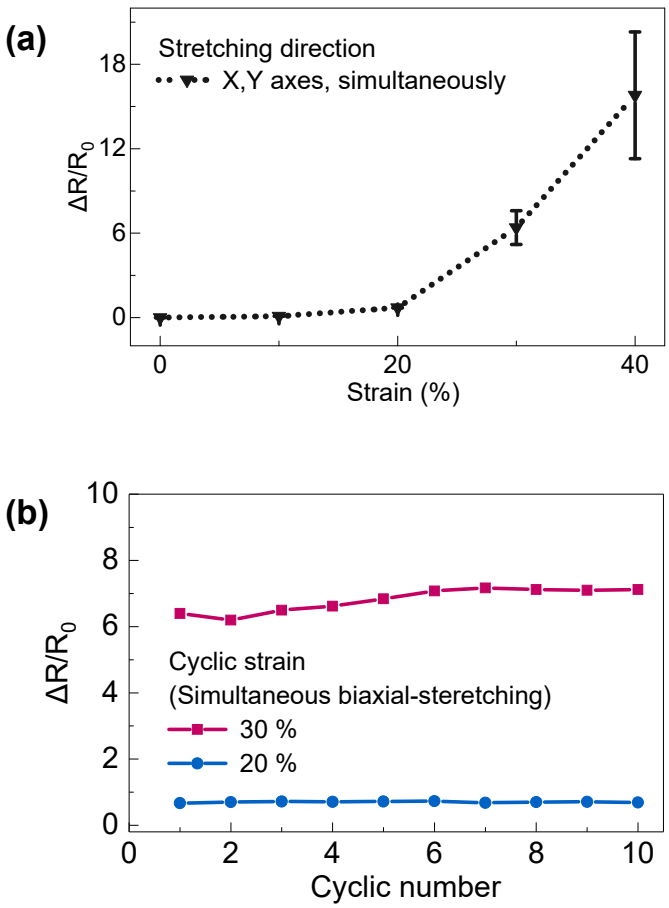

Figure S8. The biaxial stretchability and durability of the electrode. The relative resistance change ($\Delta R/R_0$) in the stretchable electrodes under (a) simultaneous biaxial stretching test and (b) the cyclic strain (20 and 30 %) test.

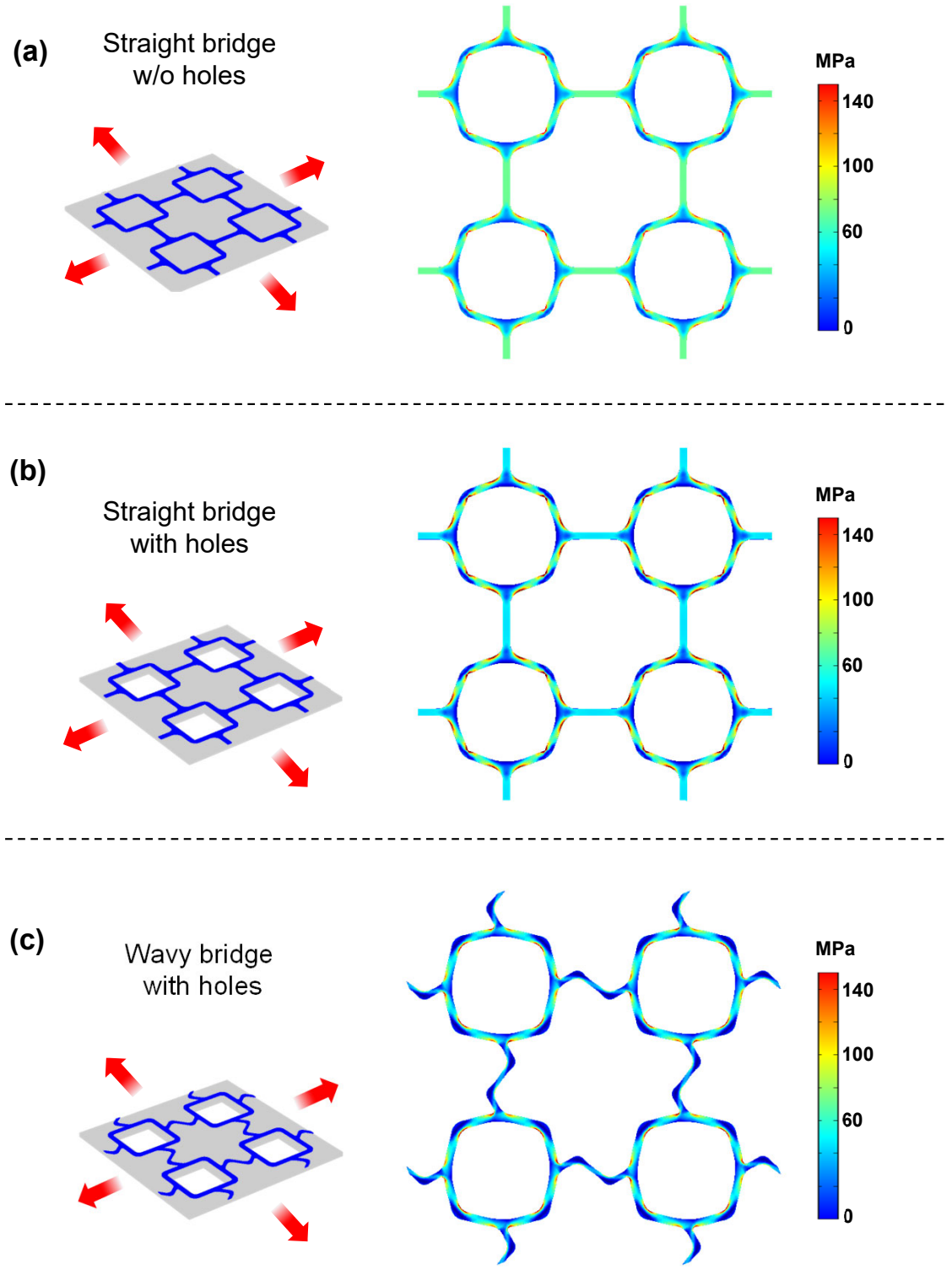

Figure S9. Simulation data of stress on and structure deformation of stretchable electrodes depending on the hole array and the structure of bridges under 20 % stretching per each X and Y axis simultaneously.

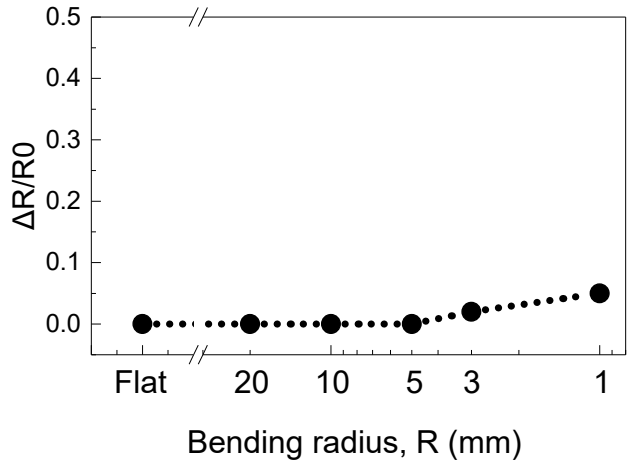

Figure S10. The relative resistance change ($\Delta R/R_0$) in the stretchable electrodes depending on the curvature radii of attachment surfaces. The curved surfaces were prepared by utilizing the outer surface of various syringes and cotton swap rods.

Ref. in the main text	Fabricating process	Electrode patterns	Relative resistance change at stretching		Vapor permeability
			Uniaxial (60%)	Biaxial (40%)	
Our work	Spraying on a patterned mold	Micromesh with wavy bridges	13.2	O / 15.8	**O**
Nano Lett., 2019, **19**, 6087 **[16]**	Laser ablation	Kirigami	< 0.03	X	-
ACS Nano, 2020, **14**, 5798 **[31]**	Dipcoating	Porous film	> 1000	O / -	**O**
J. Mater. Chem. C, 2019, **7**, 9748 **[38]**	Electrospinning	Nanofiber textiles	17.7	O / -	**O**
Adv. Electron. Mater., 2020, **6**, 2000306 **[24]**	Spraying with a shadow mask	Nanomembrane	> 1000	O / -	**O**
ACS Appl. Mater. Interfaces, 2022, **14**, 57290 **[44]**	Spraying with a shadow mask	Nanocomposite with elastomer	~ 15	O / -	-
ACS Appl. Mater. Interfaces, 2019, **11**, 31210 **[42]**	Dropcasting, stencil mask	Micropattern	> 50	O / -	-
Nanotechnology, 2016, **28**, 01LT0 **[40]**	Spraying, leaf-templates	Film	~ 15 (at 50 %)	O / -	-
ACS Appl. Mater. Interfaces, 2021, **13**, 59085 **[41]**	Spraying, laser cutting	Kirigami	< 0.1 (at 50 %)	O / < 0.1 (at 50 %)	-
ACS Mater. Lett., 2021, **3**, 912 **[39]**	Electrospinning, spraying	Microfiber textiles	~ 2	O / -	**O**
Adv. Funct. Mater., 2019, **29**, 1902922 **[43]**	Agitation	Layer by layer alignment	-4.5 (at 40 %)	O/ -	-

Table S1. Comparison of the fabrication process, electrode patterns, relative resistance change at 60 % stretching (uniaxial and biaxial directions), and vapor permeability between our work and previous works for a biaxially stretchable electrode made of silver nanowires. 'O / -' in the 'biaxial' section means that the corresponding work had the possibility of biaxial stretchability but did not test the relative resistance change at simultaneous biaxial stretching. '-' in the 'Vapor permeability' section means that the work did not discuss vapor permeability or that their electrode may not have the permeability.

Ref. [No. In the main text]	Materials	Structures	Electrical stretchability	Vapor permeability ($g \cdot m^{-2} \cdot h^{-1}$)
Our work	Ag NWs /WPU	Hole pattern	> 60 %	**~ 165** [*1] (T: 31 °C, H: 30%)
ACS Nano, 2021, **15**, 9955-9966 **[28]**	Silk PEDOT:PSS Glycerol	Fiber mat	~ 200 %	**117** (T: 37 °C)
				53 (T: 20 °C)
Adv. Fiber Mater., 2021, **3**, 302 **[30]**	Au sputtered fiber mat	Fiber mat	~ 170 %	**35.42** [*2]
ACS Nano, 2020, **14**, 5798 **[31]**	PU Ag NWs	Porous film	~ 45 %	**~ 230** [*3] (T: 35 °C, H: 40%)
Adv. Mater., 2018, **30**, 1804327 **[32]**	Graphene silicon film	Porous Kirigami	~ 1000 %	**180** [*4] (T: 20 °C)
Nat. Commun., 2014, **5**, 4779 **[45]**	Au fabric silbione film	Permeable film	~ 220 %	**7 ~ 9**
Adv. Electron. Mater., 2020, **6**, 2000306 **[24]**	AgNWs + TPE	Nanomembrane	62 %	**24.17** [*5] (T: 20 °C)
ACS Appl. Mater. Interfaces, 2019, **11**, 28387 **[46]**	PI/Au/Ti/PI	Kirigami-serpentine	~ 80 %	**20**
J. Mater. Chem. C, 2019, **7**, 9748 **[38]**	AgNW/TPU	Nanofiber textiles	50 %	**9.5**
ACS Mater. Lett., 2021, **3**, 912 **[39]**	AgMW/TPU	Nanofiber textiles	> 600 %	**13.9**

Table S2. Comparison of materials, structures, electrical stretchability, conformity, and vapor permeability among our work and previous works. 'T' and 'H' represent temperature and humidity, respectively. The reference information corresponding to the earlier works is listed below.

[*1] 0.78 g per 7 days, the diameter of circular permeability area: 6 mm, [*2] ~850 $g \cdot m^{-2}$ per a day,

[*3] ~ 23 $mg \cdot cm^{-2}$ per an hour, [*4] ~ 1.8 $g \cdot cm^{-2}$ per 100 hours, [*5] ~ 580.18 $g \cdot m^{-2}$ per a day.